J. Fluid Mech. (1974), *vol.* 65, *part* 1, *pp.* 45–63
Printed in Great Britain

The structure of turbulent density interfaces

By P. F. CRAPPER† AND P. F. LINDEN
Department of Applied Mathematics and Theoretical Physics, University of Cambridge

(Received 24 August 1973)

The structure of density interfaces upon which turbulent motions have been imposed is investigated in the laboratory. Particular attention is paid to the profiles of density across such interfaces, and the temporal response of the interface to the imposed turbulence. Interfaces over a range of Péclet numbers and Richardson numbers are examined. It is found that the interface thickness h/l (non-dimensionalized with respect to the length scale l of the turbulence) is a function of the Péclet number but independent of the Richardson number. At low Péclet numbers ($Pe \lesssim 200$) molecular diffusion is important in the determination of the interface structure and a diffusive core (across which all transport occurs by molecular diffusion) is formed in the centre of the interface. At higher Péclet numbers the interface structure appears to be determined by non-diffusive processes and h/l becomes approximately constant at a value of about 1·5. Some information concerning the intermittent nature of the mixing process at high Péclet number is obtained from records of salinity fluctuations measured at a fixed point. Finally, the implications of these data concerning the interpretations of the measurements of entrainment across an interface made by Turner (1968) are discussed.

1. Introduction

The study of mixing across a density interface is one of the more simple, yet seemingly fundamental, aspects of the more general phenomena associated with turbulence in a stably stratified fluid. Two recent and excellent reviews of turbulence in stably stratified fluids have been provided by Thorpe (1973) and Turner (1973); both these authors point out that density interfaces (i.e. regions of high density gradient compared with the bulk of the fluid) are common in nature and often appear in laboratory experiments, even when attempts have been made to ensure that the fluid remains uniformly stratified. What then are the distinguishing features of these interfaces? Under what circumstances do they form and what are their properties?

So far the work reported in the literature has dealt with the bulk transports across these interfaces (Rouse & Dodu 1955; Lofquist 1960; Turner 1968). In this paper we have attempted to take this work one stage further by looking in some detail at the structure of a density interface separating two turbulent layers. Earlier work, particularly that of Turner (1968), has shown that the

† Present address: Department of Mechanical Engineering, University of Toronto.

presence of turbulence in the layers on either side of the interface produces a marked increase in the transport across the interface of the scalar quantity producing the density difference. Turner was able to relate this transport, defined as an entrainment velocity u_e, to a Richardson number Ri based on the r.m.s. velocity u and integral length scale l of the turbulent motions near the interface and the density difference $\Delta\rho$ across the interface. He found that for large Ri the rate of entrainment across an interface stratified by temperature was greater than the entrainment rate when the density difference was produced by salt. As the molecular diffusivity of heat κ_T is much larger than that of salt κ_S ($\tau = \kappa_S/\kappa_T \approx 0{\cdot}01$) his results suggest that the rate of entrainment depends on the Péclet number $Pe = ul/\kappa$ of the flow as well as on Ri. Linden (1973) has produced a mechanistic description of the mixing process at high Pe which accounts for the observed entrainment rate for salt, but as yet the heat entrainment rate has not been explained. The measurements to be presented in this paper indicate, at least in a qualitative way, why the measured flux of heat across an interface due to turbulent mixing differs from that of salt at high Ri.

The turbulence in Turner's (1968) experiments was produced by the vertical oscillation of one or two horizontal grids. Although the structure of the turbulence is probably strongly related to the geometry of the grids, and the Reynolds number of the turbulence (based on a typical eddy diameter and velocity scale) is rather low (≈ 50), his experimental set up is a very convenient and useful one. It allows the velocity and length scale of the turbulence and the density difference $\Delta\rho$ to be set independently, and it permits quasi-steady mixing experiments to be carried out. An additional feature of the motion produced by the grids is that there is no significant mean flow in the tank (Thompson 1969); this has obvious advantages for laboratory work but must be considered with caution when trying to apply the results to situations where a mean flow is present.

In this paper we investigate the structure of an interface when turbulent motions generated by oscillating grids are imposed upon it. The measurements consist of temperature and salinity profiles through the interface and of oscillations of the interface recorded at a fixed point. In this way we determine the properties of the interface for a range of Richardson and Péclet numbers, the latter facilitated by the different molecular diffusivities of heat and salt. Although the results can be discussed in terms of these parameters we first present those for the temperature interfaces separately from those for the salinity interfaces in § 3. In § 4 the results for the two types of interfaces are compared and general conclusions regarding the structure of an interface for given Ri and Pe discussed. Finally, the measurements of entrainment across such interfaces made by Turner (1968) are reviewed in the light of these conclusions.

2. The experimental method

The experiments were carried out using the same apparatus as that used by Turner (1968); for the details of the apparatus the reader is referred to his original paper. The main addition required for our experiments was the instrumentation

which allowed profiles of temperature and salinity to be made. The temperature was measured using a copper–constantan thermocouple, one junction being traversed vertically whilst the other was kept in a constant-temperature bath. Salinity was measured using a single-electrode conductivity probe. The junction for the thermocouple gave a vertical resolution of about 0·1 cm; the conductivity probe, made from platinum wire 0·0125 cm in diameter, also had a vertical resolution of 0·1 cm. The probes were traversed by a screw-mounted trolley attached to a frame separate from the tank, the depth being recorded from the output of a linear potentiometer driven by the screw.

The data were digitized immediately and temporarily stored in the core memory of a PDP8/I computer. Later the complete digital record of the profile was stored on magnetic tape. The four-channel analog/digital converter (ADC) required an input in the range 0– + 10 V and the signals from the thermocouple and conductivity probes were amplified appropriately. The accuracies of the temperature and salinity measurements were found to be 0·3 % and 0·1 % of the full-scale reading, respectively. The computer and the equipment used are described in greater detail in Crapper (1973).

The general procedure for setting up an experiment was as follows. The tank was filled with two layers of fluid, and then stirring at the desired rate was commenced. In each particular experiment the density step was produced by either heat or salt: at no time were the effects of heat and salt variations considered together. Profiles of either temperature or salinity were taken at discrete intervals by driving the probe downwards at approximately 5 cm/s. The probe output was recorded at specified time intervals (usually 0·01 s) for 2·56 s, giving a profile of approximately 12 cm in vertical extent. Oscillations of the interface were also recorded by measurements made at a fixed point as functions of time. Measurements were taken over a period of time during which the mean value of the salinity at the point did not vary significantly. In general this meant that the records were limited to about 2 min in length, although in some circumstances longer measuring periods were used.

Apart from the special geometry of the experimental arrangement, the other major defect of this set up is that the experiments were not steady in time. However, the rate of change of $\Delta\rho$ with time was very slow and even when the entrainment was most vigorous (small $\Delta\rho$ and high stirring rates) a typical change of 0·001 g/ml in $\Delta\rho$ took approximately 60 min. Consequently, even measurements taken over a period of 2 min can be considered as representative of the quasi-steady structure of the interface.

It is most useful to relate the structure of the interface to the mean properties of the turbulent motions and the density difference across the layers. Thompson (1969) measured, using a hot-film probe, the structure of the turbulence produced by the stirring grids used in our experiments oscillating in a homogeneous fluid. His measurements show that the turbulence decays with increasing distance from the grid, and that at any given distance from the grid the r.m.s. velocity u of the turbulence is proportional to the frequency of grid oscillation. He also measured an integral scale l of the turbulence, based on the autocorrelation of the velocity measurements, and found that at the interface $l \approx 1$ cm

(independent of the stirring frequency) for the geometry used in our experiments. Using his data for the velocity and length scales at the interface, then it is possible to define the following non-dimensional parameters of the motion: a Richardson number $Ri = g\Delta\rho l/\rho u^2$, a Péclet number $Pe = ul/\kappa$ and a Reynolds number $Re = ul/\nu$. It is emphasized that the values of Pe and Ri quoted for an experiment are those appropriate to the turbulence in the vicinity of the interface. In the following attention is restricted to the effects produced by variations in Ri and Pe, as the value of Re remains approximately constant at about 50 in these experiments.

3. The experimental results

Profile measurements

Temperature interface. A series of temperature–depth profiles for various values of Ri and Pe is shown on figure 1. (As displayed here the origins of both the temperature and depth scales is arbitrary, although the centre of the interface corresponds to a depth mid-way between the grids.) It is seen that all the profiles show two well-mixed layers (except where explicitly stated otherwise, the layers on both sides of the interface are turbulent) separated by a region of essentially constant temperature gradient. At the edges of this region of linear temperature variation (which is, therefore, to a good approximation a region of constant density gradient) the temperature gradient goes smoothly to zero. The profile in figure 1 (*a*) shows an inversion at the edge of the gradient region, presumably due to a mixing event taking place. The four profiles shown are displayed in order of decreasing Pe, and it should be noted that the thickness of the constant-gradient region increases as Pe decreases. Further quantitative evidence of this dependence of the interface thickness on the Péclet number will be given below, but first we consider the question of whether these 'instantaneous' temperature profiles are representative of the temperature structure.

One piece of evidence that they are representative is provided by the compari- of mean and instantaneous profiles shown on figure 2. The mean profile was determined by recording the temperature at a fixed point as a function of time and averaging over the measurement period (approximately 50 s). Figure 2 shows two such comparisons at the same Péclet number but for different values of Ri. The close agreement between the mean and instantaneous profiles is typical particularly at large Ri. At smaller values of Ri discrepancies between the two profiles such as that shown on figure 2 (*b*) are sometimes observed. However, the difference between the estimates of the interface thickness based on the instantaneous and mean profile is within the scatter of estimates taken from repeated instantaneous profiles. This fact implies that the vertical structure of the interface varies with time at a fixed horizontal position by only a small amount: the details of this temporal variation will be discussed more fully below when the results of temperature measurements at a fixed point as a function of time are presented. It therefore seems reasonable to conclude that the results taken from instantaneous temperature profiles provide a satisfactory description of the interfacial structure.

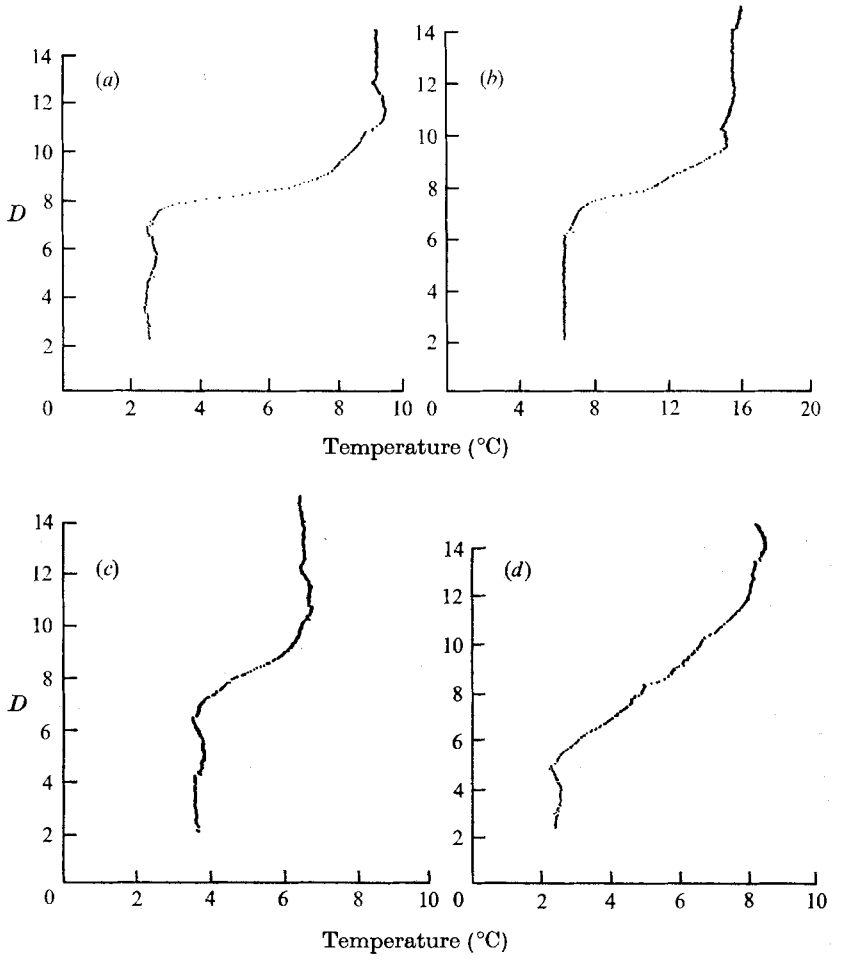

FIGURE 1. Instantaneous profiles of temperature *vs.* depth for four different values of Ri and Pe. Note the increased sharpness of the interface as the Péclet number increases. These profiles, and those shown in the following figures, are direct reproductions from the unsmoothed data as displayed on the graphics system of the PDP8/I computer, the temperature scale is in °C and the depth scale D is in cm, with the origin set arbitrarily for a convenient display. (*a*) $Ri = 32$, $Pe = 200$. (*b*) $Ri = 62{\cdot}5$, $Pe = 150$. (*c*) $Ri = 33$, $Pe = 108$. (*d*) $Ri = 416$, $Pe = 43$.

In order to quantify the profiles it is necessary to define an 'interface thickness'. This was achieved by least-squares fitting a straight line to the central 50% of the data points in the interface and extending this line until it intersected the mean temperatures of the upper and lower layers. The distance between these two intersections was defined as the interface thickness h. The central 50% of the data points were determined by considering these points whose temperature was in the range $(T_L + \frac{1}{4}\Delta T,\ T_U - \frac{1}{4}\Delta T)$, where $T_{L(U)}$ is the mean temperature of the lower (upper) layer and ΔT is the temperature difference between the layers. In all cases this procedure meant that more than 20 points were included in the least-squares fit. The fitting of a straight line to the central portion of the

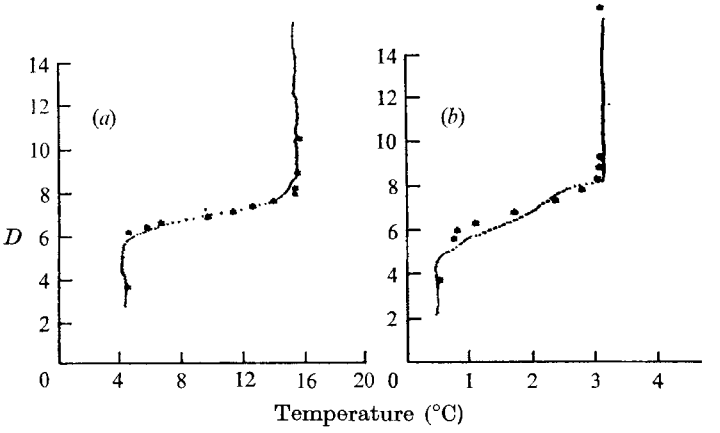

FIGURE 2. A comparison of mean and instantaneous temperature–depth profiles. (*a*) $Ri = 90$, $Pe = 155$. (*b*) $Ri = 24$, $Pe = 155$.

interface proved to be satisfactory as the difference between the values of the interface thickness calculated when the central portion of the data was fitted by a straight line and a quadratic was found to be negligible.

A further check on this estimate of the interface thickness was provided by examining a shadowgraph of the interface, three examples of which are shown on figure 3 (plate 1). Figures 3(*a*) and (*b*) show temperature interfaces for two sets of values of Ri and Pe. From photographs such as these it is possible to obtain a rough estimate of the position of the edges of the upper and lower well-mixed layers and hence the interface thickness. It was found that the visual estimate was in good agreement with that determined from the profile. Figure 3(*a*) shows a relatively thick interface similar to that shown on figure 1(*c*) whilst figure 3(*b*) exhibits a sharp interface such as that shown on figure 1(*a*). Figure 3(*c*) shows a salinity interface and will be described in more detail below.

The profiles shown on figure 1 indicate that h is a function of the Richardson and Péclet numbers. In order to determine this functional relationship we show on figure 4 a plot of h/l as a function of Ri for a fixed value of Pe. The data show no significant trend over the range of Ri although the values do tend to become slightly less at lower Ri. At these smaller values of Ri the interface is less stable and this is reflected in the increased scatter in the individual values of h/l. The data shown on this figure represent the most systematic coverage of the available Ri range (for fixed Pe) with a temperature interface. Data for other fixed values of Pe (not shown explicitly here) also exhibit no significant trend with Ri, a feature which is implicit in the presentation of the data shown on figure 5. This figure shows the values of h/l plotted for six discrete values of Pe (determined by discrete oscillation frequencies of the grids) for a temperature interface; each point represents the mean of all the values of h/l taken at a particular Pe irrespective of Ri and the error bars represent two standard deviations about the mean. As can be seen the interface thickness is determined by the Péclet number alone, decreasing as Pe increases up to the maximum value of 211 attained in these experiments. The fact that for a particular value of Pe

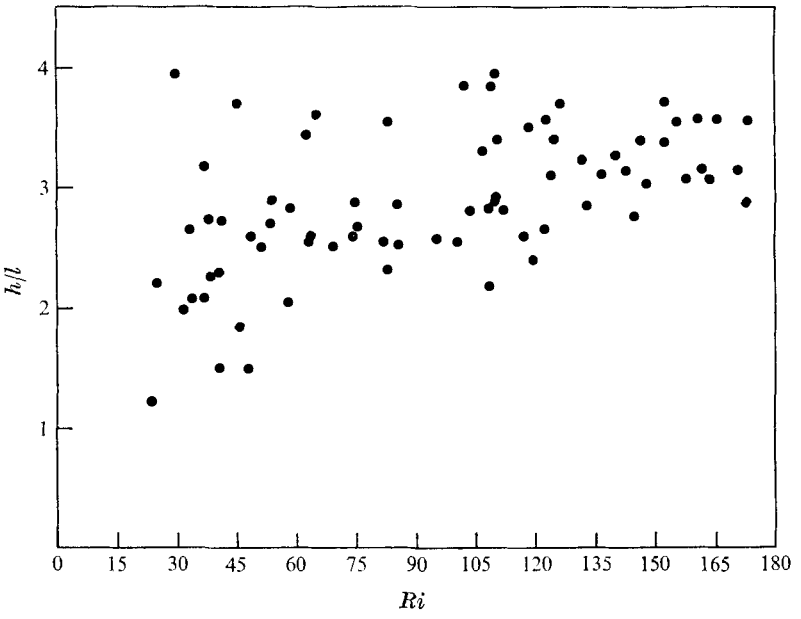

FIGURE 4. The non-dimensional interface thickness h/l plotted against the Richardson number for fixed Péclet number ($Pe = 155$).

the individual values of h/l for all Ri in the range are grouped about the mean to within the scatter due to the interface motions (i.e. the scatter in the values for fixed Ri and Pe) demonstrates that $h = h(Pe)$ for $4 < Ri < 1{\cdot}5 \times 10^3$ and $42 < Pe < 211$. For $Pe \approx 200$ (the maximum value attained for a temperature interface) $h/l \approx 1{\cdot}3$. This situation is shown on figure 3(*b*), where the turbulent eddies from each side of the interface appear to penetrate through the interface and interact directly with the layer on the other side, in contrast to the lower Pe case, where there appears to be a relatively undisturbed central region in the interface as seen on figure 3(*a*). The structure of the interface for even larger values of the Péclet number ($Pe \sim 10^4$) will be discussed below in the context of a salinity interface.

Although most of the runs were carried out at a fixed stirring rate in order to ensure statistically steady turbulent motions in the tank, in some cases the frequency of the grid oscillation was varied during a run. In these circumstances it was possible to investigate the time-dependent formation of these interfaces. In each case the interface was observed to equilibrate in a few minutes to an approximately steady state appropriate to the new stirring frequency. On figure 6 the non-dimensional interface thickness is plotted against the time elapsed since the stirring rate was changed. In each case the stirring rate was decreased from its initial value and thickening of the interface was observed; the values of h are non-dimensionalized with respect to the value h_0 of the interface thickness when the stirring rate was changed. Although the data are sparse they indicate two things: first, that in the absence of stirring ($Pe = 0$) the rate of growth is proportional to $t^{\frac{1}{2}}$ as shown by the straight line on figure 6 with slope $\frac{1}{2}$ fitted to

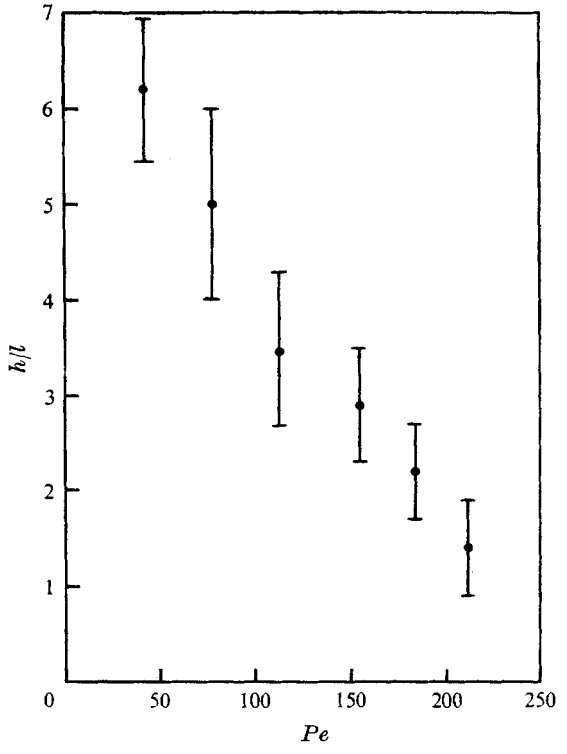

FIGURE 5. The non-dimensional interface thickness h/l plotted against Pe for temperature interfaces. The points plotted represent the mean of all values of h/l obtained at a particular value of Pe irrespective of the Richardson number (in the range $4 < Ri < 1{\cdot}5 \times 10^3$). The error bars indicate two standard deviations about this mean value.

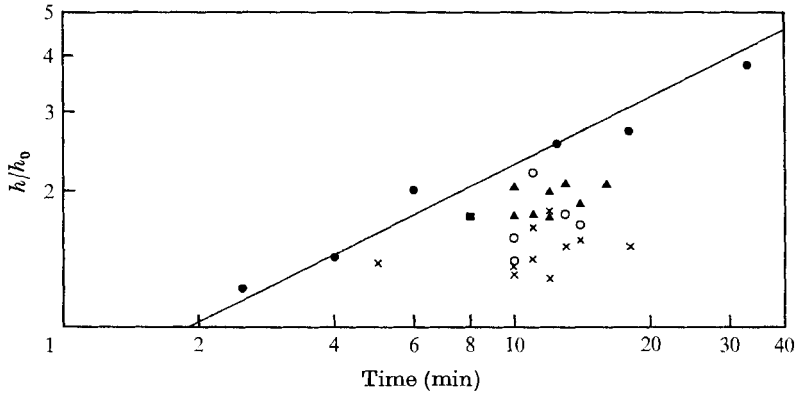

FIGURE 6. The interface thickness plotted against the time elapsed since the stirring rate was changed. The values of the interface thickness h are non-dimensionalized with respect to their initial value h_0. The full line shows a growth in interface thickness proportional to $t^{\frac{1}{2}}$, indicating that for $Pe = 0$ the spreading occurs by molecular diffusion. ●, $Pe = 0$; ▲, $Pe = 42$; ○, $Pe = 78$; ×, $Pe = 113$.

the log–log plot of the data for $Pe = 0$. This result is in accordance with the notion that the interface spreads by molecular diffusion. Taking an idealized initial temperature distribution of the form

$$T = \begin{cases} \Delta T_0, & 0 < z < \infty, \\ 0, & -\infty < z < 0, \end{cases}$$

then after time t molecular diffusion implies that the distribution is

$$T = \tfrac{1}{2}\Delta T_0 \operatorname{erfc}(-\tfrac{1}{2}z/(\kappa_T t)^{\frac{1}{2}}).$$

As a measure of the interface thickness we consider the value of $\frac{1}{2}z/(\kappa_T t)^{\frac{1}{2}}$, for which $T(z) - T(-z) = 0{\cdot}9\Delta T_0$. Then using the straight-line fit shown on figure 6, we find $\kappa_T \approx 1{\cdot}2 \times 10^{-3}$ cm^2/s; this value compares satisfactorily with the value of the coefficient of molecular diffusion of heat $\kappa_T = 1{\cdot}42 \times 10^{-3}$ cm^2/s. Second, the results show that, for $Pe \lesssim 155$, the rate of spreading of the interface, although slightly reduced by the stirring, is comparable with that produced by pure diffusion.

Salinity interface. Figure 7 shows a series of salinity interfaces for varying Ri and Pe; note that the profiles have a marked similarity in form to those taken across temperature interfaces, with the same features indicating the well-mixed layers and a central region of constant density gradient. (As with the temperature profiles the origin of the depth scale is arbitrary: the output from the conductivity probe is converted directly to density by calibration.) Figure 7 (*b*) shows a profile through an interface where only one layer (the top) is turbulent. In this case, by suitably adjusting flows into and from the layers, the interface was kept at a constant distance from the grid throughout the experiment. Note that the interface is now asymmetric with the transition from the region of constant density gradient to the uniform layer being much sharper on the turbulent side. Figure 7 (*d*) shows a comparison between an instantaneous salinity profile and a mean profile determined in the same way as the mean temperature profiles described earlier. The close agreement between the two profiles is typical. In some cases the mean profiles showed some broadening at the edges of the constant-gradient region due to fluctuations in the salinity there but in general this effect was negligible. The close correspondence between the two profiles (as was found with temperature interfaces also) indicates that the interface does not oscillate vertically with significant amplitude, a result which is in agreement with the shadowgraph observations.

It is clear from figure 7 that there is little variation of the interface thickness h (defined in the same way as that for a temperature interface) with Ri or Pe; all the salinity interfaces showed a constant value of h/l of about 1·5. Figure 8 shows the results of the instantaneous salinity profiles in terms of the non-dimensional interface thickness h/l against the Péclet number Pe. The data show that h/l is independent of Ri, which varied between 4 and 6×10^3, a result which was also found to apply to the temperature interfaces. However, at these higher values of Pe ($\sim 10^4$) h/l is also found to be independent of Pe in contrast to the large variations in h/l found at lower Pe for the temperature interfaces.

In order to determine whether the salinity interfaces were in a quasi-steady

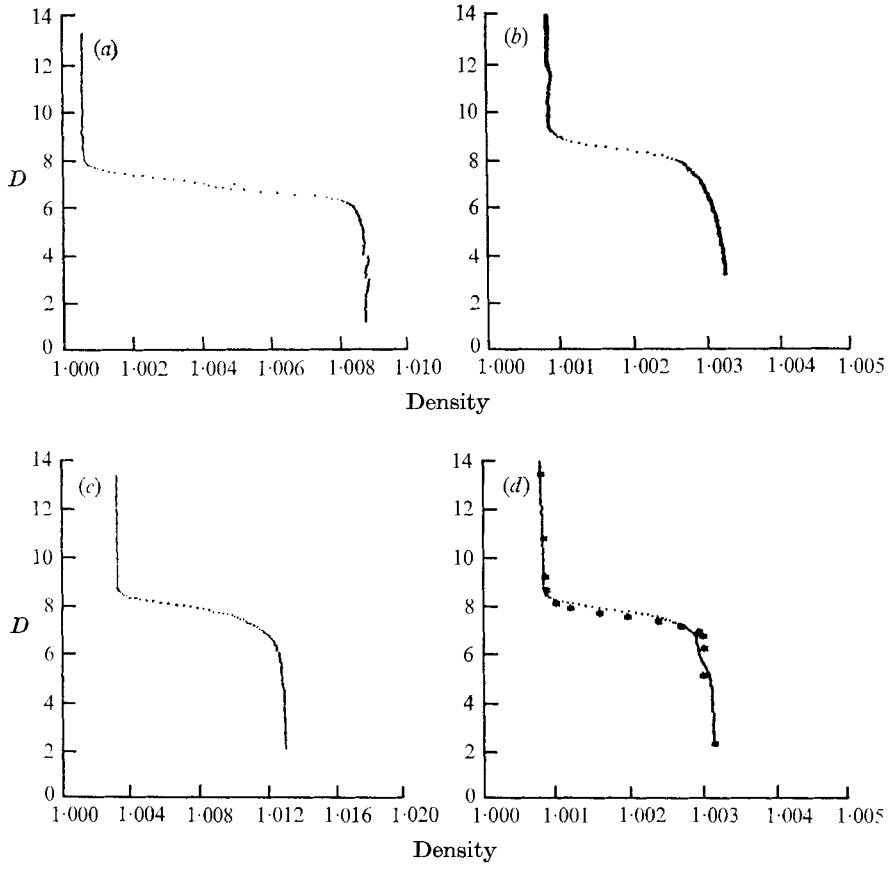

FIGURE 7. Instantaneous profiles of density, produced by salinity variations, *vs.* depth for varying values of Ri and Pe. In (*a*), (*c*) and (*d*) both layers are turbulent; in (*b*) only the top layer is turbulent. (*d*) shows a mean profile superimposed on an instantaneous profile, the mean determined by averaging readings taken over 110 s at each point. (*a*) $Ri = 8000$, $Pe = 3300$. (*b*) $Ri = 1200$, $Pe = 3300$. (*c*) $Ri = 300$, $Pe = 16000$. (*d*) $Ri = 20$, $Pe = 20000$.

state (they cannot be completely steady in our experiments as $\Delta\rho \to 0$ with increasing time), the experiments were occasionally started with a thick interface between the layers. This was achieved by letting the initial density step introduced by the filling procedure to diffuse for several days until $h \approx 10$ cm. The stirring was then begun and the time history of the interface studied by taking a series of instantaneous salinity profiles as the experiment progressed. Figure 9 shows three such profiles taken at time intervals of 30 min superimposed one upon the other. These show that the interface thickness is reduced by erosion of the edges of the gradient region by the turbulent motions in the layers. Visual observation indicated that this erosion left the central region of the interface undisturbed and the profiles shown on figure 9 show that the density gradient in the centre of the interface remains unchanged even when the edges of the interface have been significantly modified by the turbulence in the layers. It was found in each case that the thickness of the interface reduced until an equilibrium

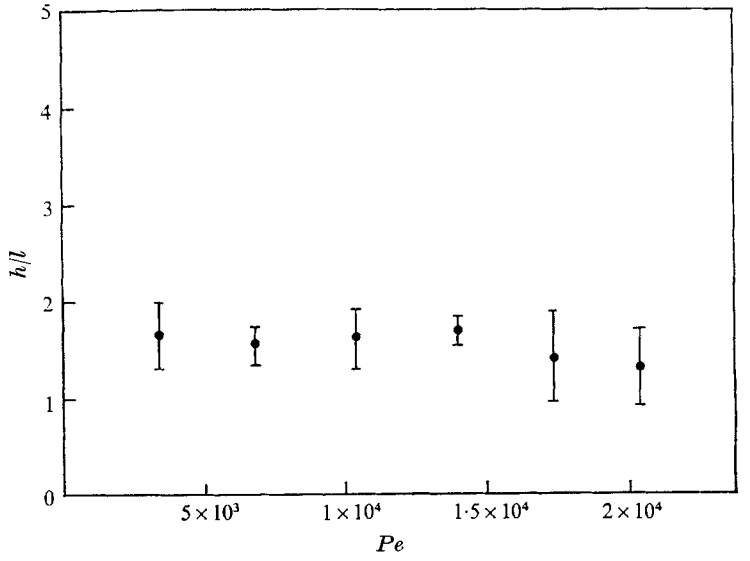

FIGURE 8. The non-dimensional interface thickness h/l plotted against Pe for salinity interfaces. The points plotted represent the mean of all values of h/l obtained at a particular value of Pe irrespective of Ri (for $4 < Ri < 6 \times 10^3$). The error bars indicate two standard deviations about this mean.

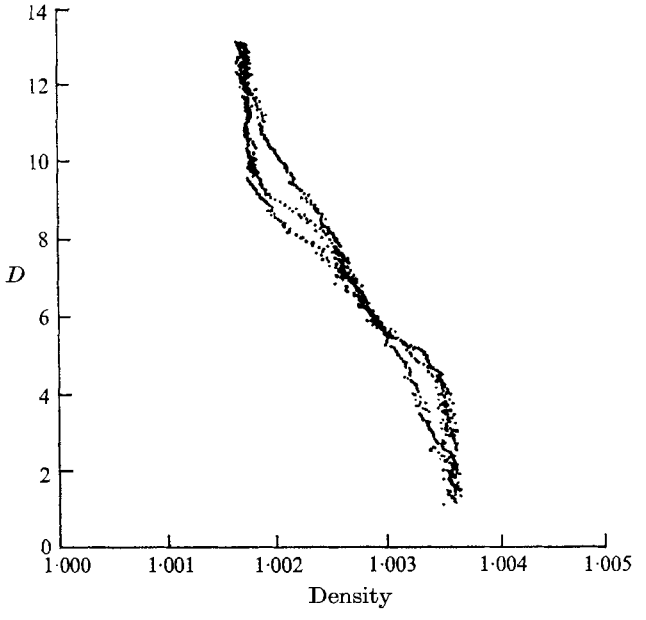

FIGURE 9. Profiles of density, produced by salinity variations, against depth taken at time intervals of 30 min for $Ri = 280$ and $Pe = 1{\cdot}5 \times 10^4$. Note the erosion of the edges of the interface by the turbulence, leaving the original gradient unchanged in the centre.

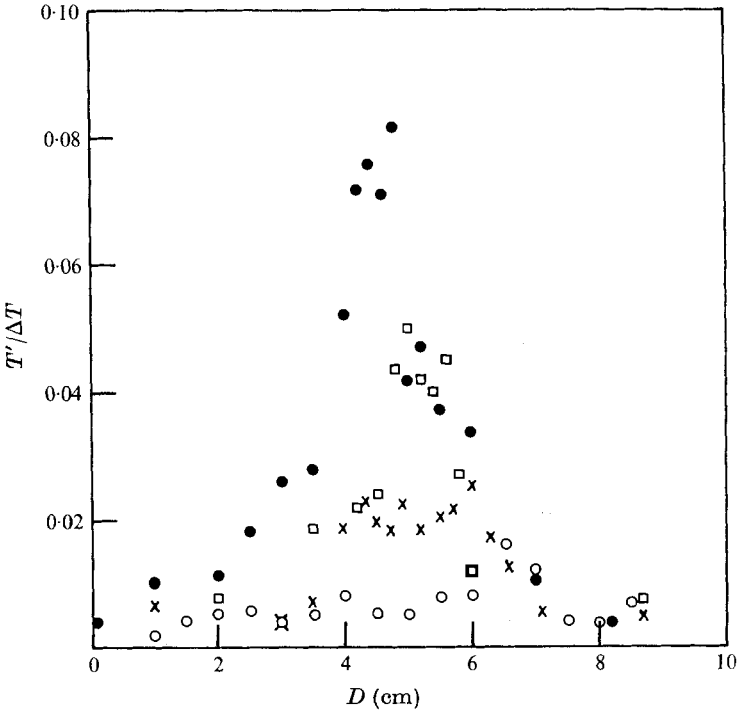

FIGURE 10. The r.m.s. value T' of the temperature fluctuations, normalized with respect to the temperature difference ΔT between the layers, plotted against the depth of the measurement point (with an arbitrary origin). ○, $Pe = 60$, $Ri = 89$; ×, $Pe = 78$, $Ri = 93$; □, $Pe = 155$, $Ri = 75$; ●, $Pe = 211$, $Ri = 72$.

situation was reached and the interface thickness remained at its 'steady' value. The rate at which the erosion by the turbulence takes place was found to increase as Ri decreases (i.e. as the interface stability decreases); however, the value of the equilibration thickness is the same in each case consistent with the data shown on figure 8.

Measurement of fluctuations at a fixed point

Temperature. Measurements of temperature at a fixed point were made in order to obtain some information concerning the temporal variation of the interface. Measurements were made for the six values of Pe mentioned above in connexion with the profile measurements and for $4 < Ri < 210$. In general readings were taken every 0·1 s for 51·2 s; the probe was then moved vertically to a new depth and the next record taken. Figure 10 shows the r.m.s. value T' of the temperature fluctuations taken from such records, non-dimensionalized with respect to the temperature difference ΔT between the layers, for various values of Pe and Ri, plotted against the depth of the measurement point. From the data displayed on figure 10 the following points should be noted. First, the magnitude of the fluctuations is at most about 0·1 ΔT, indicating that the interface does not undergo vertical oscillations comparable in height with the interfacial thickness: this

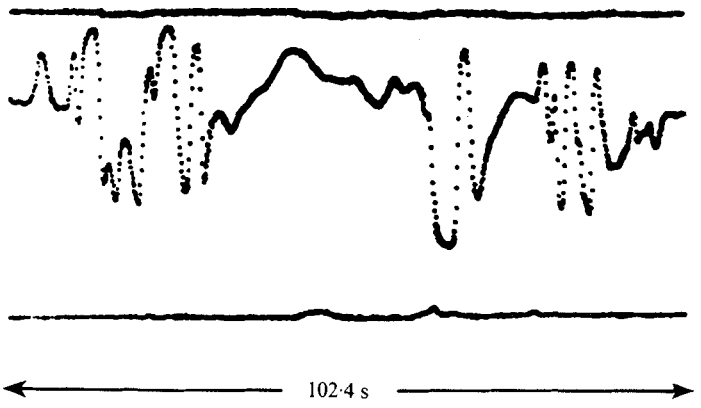

FIGURE 11. Salinity at a fixed point plotted against time. Each record represents readings taken every 0·1 s for 102·4 s. The records were obtained at three points separated by 1·0 cm in the vertical; the two outer records were taken in the mixed layers whilst the central one was measured near the centre of the interface. These measurements correspond to $Ri = 34$ and $Pe = 2{\cdot}1 \times 10^4$.

result is in agreement with the shadowgraph observations. The limit $Ri \to 0$ when the temperature difference between the layers decreases to zero provides an exception to the above result. In that case large vertical oscillations of the interface were observed; however, the breakdown in that limit was not studied in detail and so all the results discussed here exclude the case $Ri \to 0$. (In fact $Ri \approx 4$ was the lower bound on the Richardson number of the flows which were studied systematically.) Second, the data shown on figure 10 provide additional evidence (along with the temperature–depth profiles) that the structure of the interface depends on the Péclet number of the flow. The form of the function relating the r.m.s. fluctuations to the depth through the interface varies in such a way that, as Pe increases, the depth range over which the magnitude of the fluctuations is significantly greater than the value in the well-mixed layers decreases. Identifying this region of larger temperature fluctuations with the constant-gradient region noted on the temperature profiles provides a consistent pair of estimates for the interface thickness. Further, we note that as Pe increases the distribution of r.m.s. fluctuations with depth becomes more sharply peaked: this trend is clearly seen in the data displayed on figure 10. The implications of this observation will be discussed below once the salinity fluctuations have been presented.

Salinity measurements. Measurements of salinity at a fixed point were made in order to obtain some information regarding the details of the mixing process at a high Péclet number interface. Measurements were taken for

$$4{\cdot}2 \times 10^3 < Pe < 2{\cdot}1 \times 10^4 \quad \text{and} \quad 4 < Ri < 6 \times 10^3.$$

The data will be presented in a manner analogous to that for the temperature fluctuations. Typical records taken at a fixed horizontal position for three different depths in the tank separated by 1·0 cm are shown on figure 11; these records consist of readings taken at 0·1 s intervals for 102·4 s. In the upper and lower traces the fluctuations are very small and these correspond to records taken in

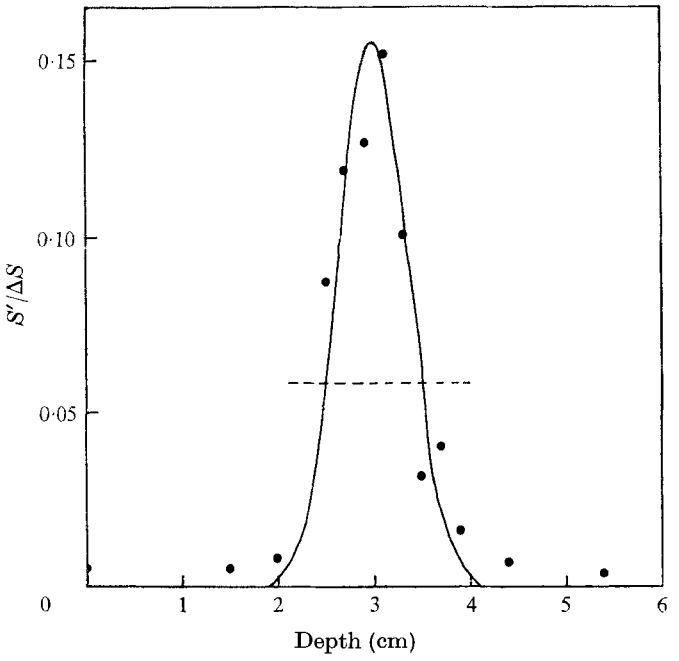

FIGURE 12. The r.m.s. value S' of the salinity fluctuations plotted against the depth at which the measurements were taken for $Pe = 2{\cdot}1 \times 10^4$ and $Ri = 81$. The magnitude of the fluctuations has been non-dimensionalized with respect to the salinity difference ΔS between the layers and the origin of the depth measurements is arbitrary. ——, Gaussian fit to the experimental data; – – –, one standard deviation of the Gaussian distribution, which has been used as a measure of the interface thickness.

the well-mixed layers on either side of the interface. The central trace, typical of one taken near the middle of the interface, shows large oscillations which appear to occur in bursts. The magnitude of these oscillations reaches some 75% of the salinity difference between the layers, indicating that fluid from both sides of the interface is being advected past the probe. For this interface $Ri = 34$, which is quite stable, and hence the large oscillations do not appear to be due to large-scale vertical motions of the interface. Such large-scale motions were *not* observed on the shadowgraph (see figure 3*c*, plate 1). The periods of these oscillations indicate that these bursts may be due to interfacial waves with wavelengths of a few centimetres forced by the turbulent motions in the well-mixed layers.

The r.m.s. value S' of the salinity fluctuations plotted against the depth of the measurement point in the tank is shown on figure 12. The magnitude of the fluctuations has been normalized with respect to the salinity difference between the layers. A Gaussian curve was fitted to the points (shown as the full curve on figure 12) and the standard deviation taken as a measure of the interface thickness. The depth of the maximum value of the fluctuations was found to coincide (to within $\pm 0{\cdot}2$ cm) with the centre of the interface as determined by an instantaneous salinity–depth profile. The non-dimensional interface thickness h/l was found to be approximately 1·5 and independent of Ri and Pe in agreement with that determined from the instantaneous profiles.

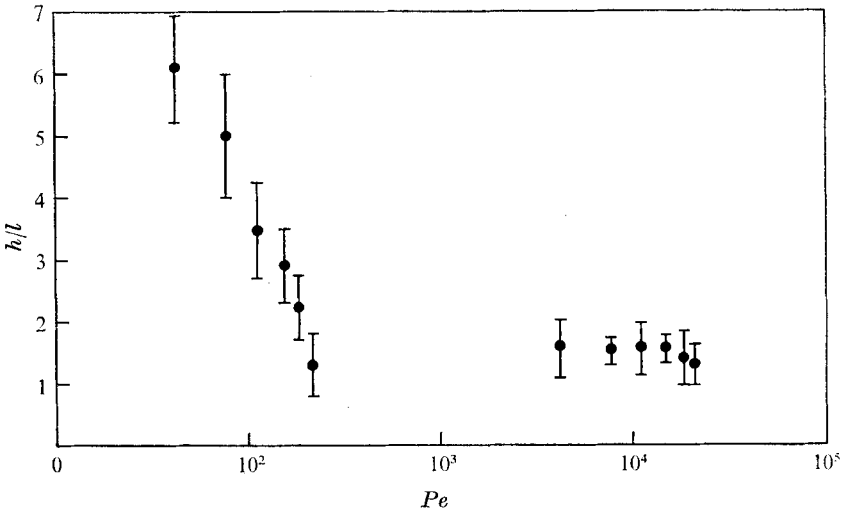

FIGURE 13. The non-dimensional thickness h/l plotted against the Péclet number. This plot is a combination of the data shown on figures 5 and 8.

4. Discussion

The measurements presented above describe certain features of a density interface in terms of the Péclet number $Pe = ul/\kappa$ and the Richardson number $Ri = g\Delta\rho l/\rho u^2$ of the flow, where l and u are the length and velocity scales of the turbulence. The experimental apparatus, which restricts attention to the case where there is no mean shear across the interface, has allowed a systematic study for Richardson numbers in the range $4 < Ri < 6 \times 10^3$ and Péclet numbers in the two distinct ranges $42 < Pe < 211$ and $4{\cdot}1 \times 10^3 < Pe < 2{\cdot}1 \times 10^4$. The Reynolds number of the turbulence $Re = ul/\nu$ was not varied in any systematic way and remained within the restricted range $10 < Re < 50$. Although the experimental data for the temperature and salinity interfaces were presented separately in § 3 it is instructive to combine the two sets of results and re-iterate the main trends.

There are two main conclusions which may be drawn from the data within the parameter ranges described above. First, the interface thickness h (non-dimensionalized with respect to the turbulent length scale l) is independent of Ri but decreases as Pe increases. As Pe becomes large ($Pe \lesssim 200$) h/l tends to a constant value of about 1·5. This result is displayed on figure 13, where the data displayed on figures 5 and 8 are combined in order to emphasize the dependence of h/l on Pe over the two ranges explored by these experiments. As Pe decreases, h/l increases and its seems to be a reasonable extrapolation of the data shown on figure 13 to suppose that $h/l \to \infty$ as $Pe \to 0$. In the limit $Pe = 0$ then, by diffusion h/l grows without bound (in an infinite container) and attains no 'steady-state' value. At the other extreme as $Pe \to \infty$ (but with $Ri > 1$, say) the data indicate that h is independent of both κ and $\Delta\rho$. Consequently, dimensional analysis implies that $h/l = f(Re)$; in these experiments Re did not vary much and so it is

not possible to comment on the form of the functional dependence on Reynolds number except to say that it must be a slowly varying function of Re as shown by the approximately constant value of h/l for $Pe \gtrsim 200$ shown on figure 13.

The second conclusion to be drawn from the data is the nature of the dependence of the r.m.s. value of the fluctuations on the depth through an interface. The results of figures 10 and 12 show that for large Pe the distribution of the fluctuations tends to a Gaussian form, and as Pe decreases the distribution becomes flattened in the middle with a more even spread of the magnitude of the fluctuations across the interface. Further, the non-dimensional magnitude of the fluctuations decreases as Pe decreases and clearly as $Pe \to 0$ the fluctuations will decrease to zero.

In order to relate these results to the measurements of entrainment across an interface we make use of one additional observation. This is the shadowgraph view of a low Péclet number interface as shown on figure 3 (*a*) (plate 1). We see that the turbulent motions in the well-mixed layers do not penetrate to the centre of the interface (in contrast to the high Pe case, figure 3*c*, plate 1). What then provides the transport of the scalar (heat in this case) across this central region? As there is no visual evidence (or from the profiles) of breaking internal waves in this region we conclude that a low Péclet number interface ($Pe \lesssim 200$) has a central 'diffusive core' across which all transport occurs by molecular diffusion. As the temperature gradient in this region is constant this implies that there is a constant vertical flux of heat across it. For the system to be in a quasi-steady state this flux must be balanced by entrainment fluxes at the edges of the layers as the temperature gradient goes to zero there, and there can be no diffusive flux. This balance between entrainment and diffusion must also determine the value of h/l in these cases, with diffusion tending to broaden the interface and entrainment tending to sharpen it (see figures 6 and 9). Thus as the Péclet number, and hence the turbulent transport, increases the interface tends to sharpen. This increases the gradient in the central region and hence the diffusive flux until a balance is re-established. With further increase in Pe eventually a situation will be reached when molecular diffusion cannot balance the entrainment flux and direct mechanical transport of fluid across the interface will occur (see, for example, figure 3*c*).

This picture is confirmed by observations of the distribution of the r.m.s. fluctuations with increasing Pe. At low Pe the distribution is relatively flat (figure 10), indicating that the diffusive core is responding to forcing by the turbulence with motions of about the same vertical scale throughout its depth. This is consistent with internal waves propagating in the core. At the edges of the core the temperature gradient is small and so much larger oscillations (due to impingement of turbulent eddies) can cause only similarly scaled temperature fluctuations. As Pe increases the flatness of the distribution decreases, indicating a reduction of the diffusive core; at very large Pe ($\sim 10^4$) the distribution becomes approximately Gaussian and there is no evidence of a diffusive core.

So far the hypothesis of a diffusive core has only been shown to be plausible. In order to show that it is a real feature of a low Pe interface it is necessary to

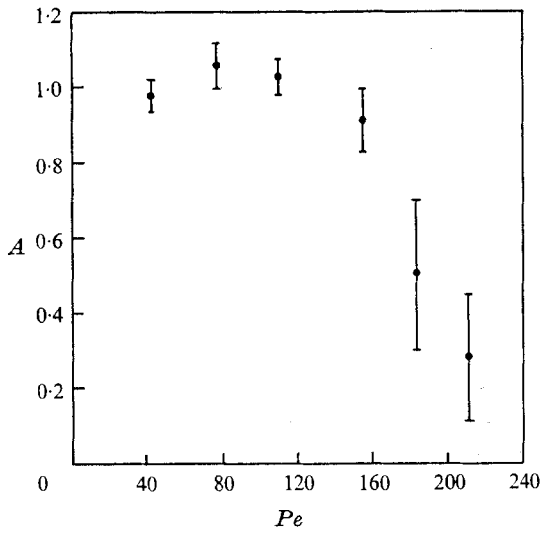

FIGURE 14. The ratio A of the observed flux across the interface to that produced by diffusion down the observed gradient in the interface plotted against the Péclet number Pe.

demonstrate that the observed gradients can support a diffusive flux comparable with that which is measured. Figure 14 shows a comparison of the total flux as measured by monitoring the density difference between the layers as a function of time and the diffusive flux as estimated from the observed density gradient plotted as a function of Pe. We see that for $Pe \lesssim 100$ the diffusive flux is approximately equal to the entrainment flux, whilst for $Pe \gtrsim 200$ the fraction decreases significantly. For $Pe \gtrsim 200$ it is no longer possible to balance the transport by diffusion and direct mechanical transport of fluid from one side of the interface to the other is necessary to provide the observed entrainment rates.

The experiments described in this paper provide little information on the nature of the entrainment process at high Pe. The records of salinity at a fixed point as a function of time indicate that the mixing process occurs in bursts, possibly due to the impingement of a turbulent eddy on the interface, and that a point on the interface may be subject to one such 'event' about every 100 s. This is in agreement with an implication of the results of the flux measurements of Turner (1968) that the turbulence on both sides of the interface is decoupled in the sense that the arrival of two eddies of the interface at the same place and at the same time is a rare event.

Another striking feature of the high Péclet number interface is the fact that the interface thickness remains at a constant value independent of Pe and Ri. Clearly, the interface thickness at large Pe must result from some form of balance between the tendency of the turbulence to erode the edge of the interface and the tendency of mixed fluid to remain near the interface because of its intermediate density. How this balance is achieved, however, is not clear. Unfortunately, the geometry of the experiments was such that it was not possible to vary l significantly: the fact that, at high Pe, $h \approx l$ may just be a coincidence. (A further note of caution should be added to such an interpretation as the

measurements of l were made with a homogeneous fluid in the tank. The effect of density gradients on l has not been evaluated although some experiments with vortex rings incident on density interfaces by Linden (1973) indicate that l should not vary too much from the homogeneous case.) The results do show, however, that h is not determined by a 'critical Richardson number' criterion, where the gradient Richardson number $Ri' = g\Delta\rho h/\rho u^2$ is kept at a constant 'critical' value owing to shear instability of the interface. The fact that at high Pe h/l (and therefore h) is independent of both u and $\Delta\rho$ (Pe and Ri) shows that Ri' cannot be constant if u or $\Delta\rho$ varies. The lack of this type of limit on the interface thickness in these experiments without a mean shear would appear to be one of the main disadvantages in applying results obtained with grid-generated turbulence to situations where a significant shear flow is present.

Finally, we return to a consideration of Turner's (1968) measurements of the entrainment rate across an interface made in the same tank as the experiments reported here. As was stated earlier he found that the non-dimensional entrainment rate scaled with the Richardson number of the flow but had a different functional form depending on whether a temperature or salinity interface was used. He found that at large Ri the mixing rate for heat was greater than that for salt, but that the rates were the same for $Ri \lesssim 7$. For the temperature differences he used $Ri < 7$ corresponds to $Pe > 200$ for the temperature interface. Our results show that for $Pe \gtrsim 200$ the transport across an interface takes place by mechanical entrainment, and so the fact that the heat and salt rates were observed to be the same is consistent with the idea that diffusion is unimportant in this range. At higher Ri, the Péclet number (in Turner's heat experiments) was less than 200 and so diffusion becomes important in the case of the temperature measurements. This transition from an interface across which all the transport takes place by direct mechanical entrainment to one in which a central diffusive core exists accounts qualitatively for the observed difference in the respective dependence of the entrainment rate on the Richardson number in the two cases. It does not, however, explain why the rate of entrainment should be greater at the low values of Pe (< 200) than at larger values. The presence, at low Pe, of a region of constant density gradient whose thickness is large compared with the length scale of the turbulence indicates that the turbulent eddies and possibly the entrainment mechanism itself may be significantly affected by the density gradient. However, the way in which regions of density gradient interact with turbulent motions is a problem still to be resolved.

We are grateful to Prof. H. Charnock for a discussion of this work and to the Natural Environment Research Council for financial support.

REFERENCES

Crapper, P. F. 1973 An experimental study of mixing across density interfaces. Ph.D. thesis, University of Cambridge.

Linden, P. F. 1973 The interaction of a vortex ring with a sharp density interface: a model for turbulent entrainment. *J. Fluid Mech.* **60**, 467.

LOFQUIST, K. 1960 Flow and stress near an interface between stratified liquids. *Phys. Fluids*, **3**, 158.

ROUSE, H. & DODU, J. 1955 Turbulent diffusion across a density discontinuity. *Houille Blanche*, **10**, 530.

THOMPSON, S. M. 1969 Turbulent interfaces generated by an oscillating grid in a stably stratified fluid. Ph.D. thesis, University of Cambridge.

THORPE, S. A. 1973 Turbulence in stably stratified fluids: a review of laboratory experiments. *Boundary Layer Meteor.* **5**, 95.

TURNER, J. S. 1968 The influence of molecular diffusivity on turbulent entrainment across a density interface. *J. Fluid Mech.* **33**, 639.

TURNER, J. S. 1973 *Buoyancy Effects in Fluids*. Cambridge University Press.

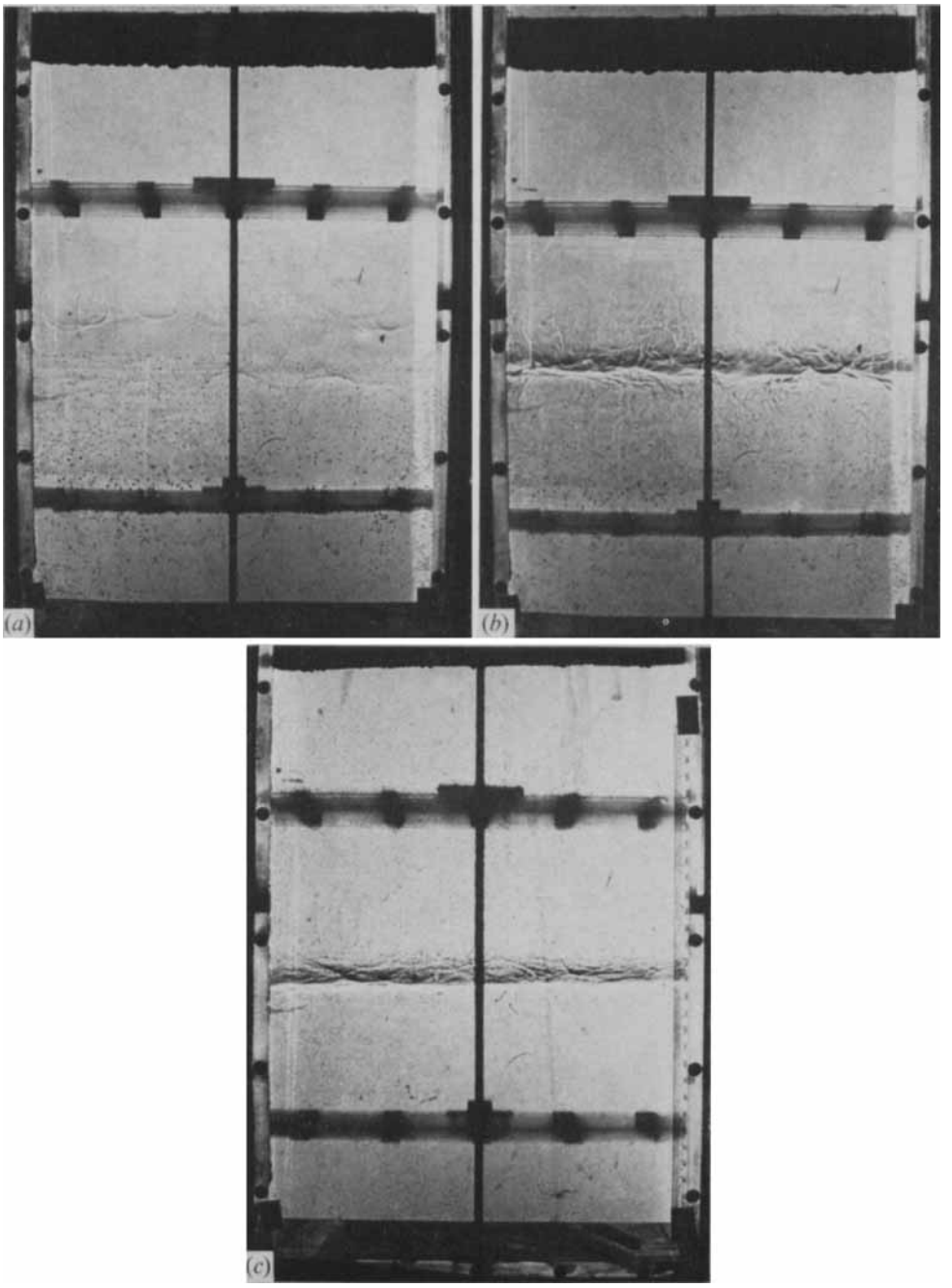

FIGURE 3. Shadowgraph views of turbulent interfaces. (*a*) $Pe = 52$, $Ri = 397$. (*b*) $Pe = 200$, $Ri = 34$. (*c*) $Pe = 2200$, $Ri = 8000$. Note the similarity between the heat and salt interface at high stirring rates in (*b*) and (*c*). The distance between the grids is 18·0 cm.